URSI GASS 2021, Rome, Italy, 28 August - 4 September 2021

Bringing numerical treatment planning for electroporation based therapies into clinical practice

Bor Kos[(1)]
(1) University of Ljubljana, Faculty of Electrical Engineering, Ljubljana, Slovenia

Abstract

Electroporation occurs when cells are exposed to sufficiently strong external electric field. This can be used to introduce therapeutic molecules inside the target cells, or to directly cause cell death. Since the electric field strength has a very inhomogeneous distribution around needle electrodes, and the difference in conductivity between various normal and malignant tissues which affects the electric field distribution even more, numerical modelling can be essential in treatment planning and development of new treatments in the field of oncology. Presentation will detail methods of treatment planning and the current state of the art.

1 Introduction

Electroporation occurs when cells are exposed to sufficiently strong external electric field. This causes a transient increase in cell membrane permeability to various ions and molecules. Depending on the number of pulses, pulse amplitude and duration, and pulse delivery frequency, electroporation can be either reversible or irreversible. Reversible electroporation is used in combination with cytotoxic drugs bleomycin and cisplatin in a treatment termed electrochemotherapy (ECT) [1]. In this treatment, 8 pulses of 100 µs duration are delivered per electrode pair, typically with a high repetition frequency. ECT is used most often in the treatment of cutaneous and subcutaneous tumors [2], but has been used successfully to treat also deep seated tumors in the liver [3]–[6], pancreas, bones and the spine [7].

Irreversible electroporation (IRE) can be used to directly ablate tissue [1], [8], which is used for treatment of solid tumors, most commonly in the liver [9]–[11], pancreas [12] and the prostate [13]. In IRE, electric pulses are typically delivered one per heartbeat, for a total of 90 pulses per electrode pair.

There are various electrode types available to the clinical users for performing ECT [14] and several fixed geometry electrodes exist, which facilitate the placement and should ensure robust coverage of the target volume with sufficiently strong electric fields, however these can only be used on the surface, or on the surface of organs in the intraoperative setting. In IRE, individual long needle electrodes are used almost exclusively [11], and the clinicians use a fixed voltage-to-distance ratio as recommended by the device manufacturer. However the electric field between needle electrodes is highly inhomogeneous and a simple voltage-to-distance ratio cannot always ensure a homogeneous coverage of the target tissue with sufficiently strong electric fields, especially due to the conductivity contrast between target tumors and surrounding healthy tissues [15].

2 Tissue properties during electroporation

It has been well documented, that tissue dielectric properties change dramatically during the process of electroporation [16], [17]. This conductivity increase is typically explained with an increase in the availability of conductive pathways through the cellular membrane, which allow the flow of current-carrying ions, for which theoretical models of pore formation have been proposed and validated for various in-vitro cell level experiments [18]. Many studies using molecular dynamics approaches also show the rapid formation of hydrophilic pores in a small section of the lipid bilayer [19].

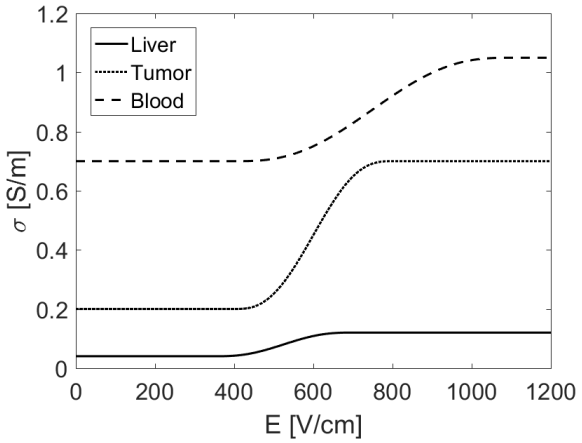

Figure 1. Examples of tissue conductivity during electroporation. Tissue properties as used in numerical study of Marčan et al [20].

This tissue conductivity change occurs rapidly, within the first few microseconds of applied electric field [16]. This also results in a modification of the local electric field strength, namely, the electric field near the electrodes is reduced, while tissue further away from the electrode surfaces experiences a higher local electric field [21]. The tissue conductivity as a function of local electric field strength is illustrated in Figure 1 for different tissues, which are affected in the treatment of liver tumors with electroporation based treatments.

3 Numerical modelling approach

Electroporation occurs, when the induced transmembrane voltage (ITV), which is induced on the cellular membrane of cells in exposed to electric fields, exceeds a threshold of approximately 500 mV. This ITV can be calculated for a spherical cell using Schwann's equation:

$$ITV = 1.5\, ER \cdot \cos(\phi) \quad (1)$$

Where E is the local electric field strength, R is the radius of the cell and ϕ is the angle measured from the center of the cell with respect to the electric field direction.

The local electric field can in most cases of realistic anatomy only be determined numerically. To do this, the Laplace equation for electric potential has to be solved:

$$\nabla \cdot (\sigma(E)\nabla V) = 0, \quad (2)$$

$$E = -\nabla V, \quad (3)$$

Where $\sigma(E)$ is the local conductivity dependent on the electric field, V is the electric potential and E is the electric field strength. These equations are most often solved using the finite element method [22], but other numerical approaches, such as finite difference method have also been used successfully [23]. Since electroporation based treatments usually employ more than one electrode pair, which are switched and the pulses are delivered to separate electrode pairs sequentially. This allows the treatment to cover a larger target volume. Although the electric field threshold for both reversible and irreversible electroporation generally decreases with number of pulses [24], the handling of multiple electrode pairs can be done as shown in equation 4:

$$E_{treatment} = \max E_i\,, \quad (4)$$

where $E_{treatment}$ is the local electric field to be compared with the defined threshold for the intended therapy, and E_i is the electric field from i-th electrode pair. This simplification presents a conservative solution, but has the benefit of not being dependent on the order of pulse delivery, which simplifies the treatment planning process. This electric field can then be input into the cost functions, which enable the comparison of different possible solutions. The numerical methods therefore allow the computation of local electric field in the entire region of interest, which therefore enables precise control over the treatment.

4 Patient specific models

Patient specific models can be derived from tomographic images – CT and MRI. Depending on the target tissue and tumor type different modalities can improve target tissue visibility and contrast from surrounding healthy or critical sensitive tissue. Tissue conductivity is not directly related to any imaging modality, so an intermediate step of tissue segmentation needs to be performed to delineate the different tissues. This segmentation can then be used to assign appropriate tissue properties to different tissues in the region of interest, and at the same time the segmentation masks can be used to determine the target tissue in which the electric field needs to be optimized.

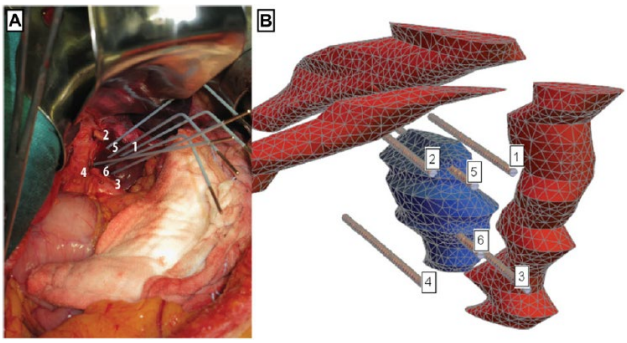

Figure 2. Patient specific treatment plan put into practice. A) Final needle position during intraoperative ECT. B) Patient specific plan showing the tumor (blue), needles (numbered 1-6), and adjacent blood vessels (red). Image from

Recently a new MRI reconstruction algorithm, which could (with appropriate reconstruction algorithms) theoretically be used on any clinical MRI scanner to directly image tissue conductivity, has been proposed [25]. This should allow the creation of anatomical, patient specific models without the intermediate step, which will also take into account the inherent inhomogeneity of tissues.

5 Optimization of the treatment plan

The patient specific models can be used, in conjunction with the numerical methods, to compute the coverage of the target volume, and surrounding tissue with sufficiently strong electric fields. This enables the use of the model to also determine areas with potential undertreatment, as well as identify critical tissues which could be endangered by the treatment. With the typical treatments with variable geometries consisting of at least 4 electrode pairs, and up to 6, which can be simultaneously connected to the pulse generator, the number of possible electrode pairs is typically between 6 and 15. Even without movement of the electrodes this presents a formidably large parameter space for the optimization. Genetic algorithms have been used previously to perform full optimization of treatment plans [22]. If electrode positions are fixed, and only voltages are optimized, a gradient algorithm can also be used.

For optimization, a cost function needs to be developed, which enables the optimization algorithm to compare different solutions. Cost functions can be formulated to maximize the target volume covered above the reversible or irreversible electroporation thresholds, and minimize the possibility of irreversible damage to sensitive structures, such as bile ducts in the liver, urethra and neurovascular bundles in the prostate, spinal cord in the vertebra, etc. Examples of such cost functions and the effect they have on the final treatment plan are shown in [22].

6 Treatment plan realization

Treatment plans need to be well executed and because the electric field strength around the needle electrodes is highly inhomogeneous, precise positioning of the electrodes is

critical. With manual placement such accuracy is difficult to achieve even under CT guidance. For more control in the placement, navigation devices can be used. Optical navigation can be registered to pre-treatment medical images, which have been used to generate the treatment plan [26]. This is also illustrated in Figure 2.

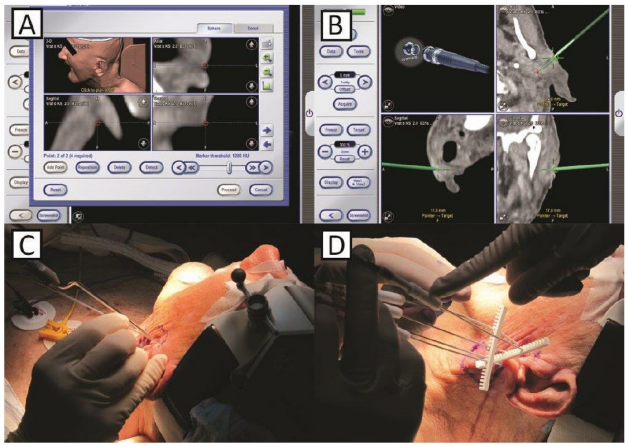

Figure 3. Positioning the electrodes for ECT of head and neck tumors using optical navigation. A) Registration of the navigation space and medical images. B) Navigation tracks defined by the treatment plannign procedure. C) Navigating the needle to the entry point. D) Final needle position during treatment. Image from **[26]**.

Also robotic and optical navigation systems have been used successfully to position electrodes for IRE treatment [11], however these work with images taken at the day of intervention, therefore using this kind of navigation would require either that the treatment plan, which was prepared in advance would be registered to the images taken at the day of the treatment, or that the treatment plan be computed on-line directly before the placement of the electrodes. The first option has the potential of working very well for tumors located in bones, or in the head region, where the anatomy is rigid, but would be more challenging in softer organs, such as the liver or pancreas. The second option would also require very quick segmentation of images and immediate computation of the treatment plan. The numerical intensity of the current models of electroporation does not yet allow this to be done quickly enough, but it could be used to provide feedback to the performing physicians by the end of the delivery of all pulses and indicate areas of potential undertreatment.

7 Regulatory requirements

Any treatment planning software provides guidance to the physician on the execution of the treatment and is therefore a medical device. The certification of medical devices is a technically challenging and time-consuming effort, and because the energies involved and also the potential to cause serious harm in case of poorly prepared or erroneous treatment plans, this kind of certification would also need to involve a notified body. The requirements for development and certification are set to become even more involved with the Regulation (EU) 2017/745 coming into force in May 2020.

The basis of medical device development is usability engineering, which details the precise requirements for the final medical device and the intended workflow. This also includes the precise definition of intended indications and expected clinical outcomes. Risk management is also an integral part of medical device development, and needs to be considered in every step of development, from usability, through software and hardware implementations. Every conceivable hazard needs to be taken into consideration, and in the analysis, every hazard's probability of occurring is estimated. If the product of hazard and probability is too high, the risk is deemed inappropriate, and measures need to be taken to reduce it. These can be in the form of use warnings or training, software checks or hardware safety devices. Finally the newly developed medical device needs to be tested in a clinical trial to demonstrate safety.

8 Conclusions

Treatment planning for electroporation based therapies is feasible and should allow for a good outcome of therapies with low dependence on operator proficiency. The treatment plans can also be executed precisely using navigation tools already deployed in clinics. In order for treatment planning to be routinely used in the everyday clinical workflow of electroporation based treatments, the demand will need to come from clinical users, and medical device manufacturers will need to develop and market it successfully.

9 Acknowledgements

The authors acknowledges funding by Slovenian Research Agency (ARRS) Program P2-0249. Study was done within Infrastructure Programme: Network of research infrastructure centers at University of Ljubljana (MRIC UL IP-0510).

10 References

[1] M. L. Yarmush, A. Golberg, G. Serša, T. Kotnik, and D. Miklavčič, "Electroporation-Based Technologies for Medicine: Principles, Applications, and Challenges," *Annual Review of Biomedical Engineering*, vol. 16, no. 1, pp. 295–320, 2014, doi: 10.1146/annurev-bioeng-071813-104622.

[2] L. G. Campana *et al.*, "Electrochemotherapy of superficial tumors - Current status:: Basic principles, operating procedures, shared indications, and emerging applications," *Semin. Oncol.*, vol. 46, no. 2, pp. 173–191, 2019, doi: 10.1053/j.seminoncol.2019.04.002.

[3] I. Edhemovic *et al.*, "Intraoperative electrochemotherapy of colorectal liver metastases," *J Surg Oncol*, Apr. 2014, doi: 10.1002/jso.23625.

[4] L. Tarantino *et al.*, "Percutaneous electrochemotherapy in the treatment of portal vein

tumor thrombosis at hepatic hilum in patients with hepatocellular carcinoma in cirrhosis: A feasibility study," *World J. Gastroenterol.*, vol. 23, no. 5, pp. 906–918, Feb. 2017, doi: 10.3748/wjg.v23.i5.906.

[5] M. Djokic *et al.*, "Electrochemotherapy as treatment option for hepatocellular carcinoma, a prospective pilot study," *Eur J Surg Oncol*, Feb. 2018, doi: 10.1016/j.ejso.2018.01.090.

[6] U. Probst, I. Fuhrmann, L. Beyer, and P. Wiggermann, "Electrochemotherapy as a New Modality in Interventional Oncology: A Review," *Technol. Cancer Res. Treat.*, vol. 17, p. 1533033818785329, 01 2018, doi: 10.1177/1533033818785329.

[7] F. H. Cornelis *et al.*, "Percutaneous Image-Guided Electrochemotherapy of Spine Metastases: Initial Experience," *Cardiovasc Intervent Radiol*, vol. 42, no. 12, pp. 1806–1809, Dec. 2019, doi: 10.1007/s00270-019-02316-4.

[8] R. Davalos, L. Mir, and B. Rubinsky, "Tissue Ablation with Irreversible Electroporation," *Ann Biomed Eng*, vol. 33, no. 2, pp. 223–231, Feb. 2005, doi: 10.1007/s10439-005-8981-8.

[9] H. J. Scheffer *et al.*, "Irreversible Electroporation for Nonthermal Tumor Ablation in the Clinical Setting: A Systematic Review of Safety and Efficacy," *Journal of Vascular and Interventional Radiology*, vol. 25, no. 7, pp. 997–1011, Jul. 2014, doi: 10.1016/j.jvir.2014.01.028.

[10] A. H. Ruarus *et al.*, "Irreversible Electroporation in Hepatopancreaticobiliary Tumours," *Canadian Association of Radiologists Journal*, vol. 69, no. 1, pp. 38–50, Feb. 2018, doi: 10.1016/j.carj.2017.10.005.

[11] L. P. Beyer *et al.*, "Stereotactically-navigated percutaneous Irreversible Electroporation (IRE) compared to conventional IRE: a prospective trial," *PeerJ*, vol. 4, p. e2277, Aug. 2016, doi: 10.7717/peerj.2277.

[12] R. C. G. Martin, P. Philips, S. Ellis, D. Hayes, and S. Bagla, "Irreversible electroporation of unresectable soft tissue tumors with vascular invasion: effective palliation," *BMC Cancer*, vol. 14, p. 540, 2014, doi: 10.1186/1471-2407-14-540.

[13] L. P. Beyer *et al.*, "Percutaneous irreversible electroporation (IRE) of prostate cancer: Contrast-enhanced ultrasound (CEUS) findings during follow up," *Clin. Hemorheol. Microcirc.*, vol. 64, no. 3, pp. 501–506, 2016, doi: 10.3233/CH-168125.

[14] D. Miklavčič, B. Mali, B. Kos, R. Heller, and G. Serša, "Electrochemotherapy: from the drawing board into medical practice," *Biomed Eng Online*, vol. 13, no. 1, p. 29, 2014, doi: 10.1186/1475-925X-13-29.

[15] B. Kos, A. Zupanic, T. Kotnik, M. Snoj, G. Sersa, and D. Miklavcic, "Robustness of treatment planning for electrochemotherapy of deep-seated tumors," *J Membr Biol*, vol. 236, no. 1, pp. 147–153, Jul. 2010, doi: 10.1007/s00232-010-9274-1.

[16] D. Cukjati, D. Batiuskaite, F. Andre, D. Miklavcic, and L. Mir, "Real time electroporation control for accurate and safe in vivo non-viral gene therapy," *Bioelectrochemistry*, vol. 70, no. 2, pp. 501–507, May 2007, doi: 10.1016/j.bioelechem.2006.11.001.

[17] A. Ivorra, B. Al-Sakere, B. Rubinsky, and L. Mir, "In vivo electrical conductivity measurements during and after tumor electroporation: conductivity changes reflect the treatment outcome," *Phys Med Biol*, vol. 54, no. 19, pp. 5949–5963, Oct. 2009, doi: 10.1088/0031-9155/54/19/019.

[18] W. Krassowska and J. C. Neu, "Response of a single cell to an external electric field," *Biophysical Journal*, vol. 66, pp. 1768–1776, 1994.

[19] L. Delemotte and M. Tarek, "Molecular dynamics simulations of lipid membrane electroporation," *J. Membr. Biol.*, vol. 245, no. 9, pp. 531–543, Sep. 2012, doi: 10.1007/s00232-012-9434-6.

[20] M. Marčan, B. Kos, and D. Miklavčič, "Effect of blood vessel segmentation on the outcome of electroporation-based treatments of liver tumors," *PLoS ONE*, vol. 10, no. 5, p. e0125591, 2015, doi: 10.1371/journal.pone.0125591.

[21] D. Sel, D. Cukjati, D. Batiuskaite, T. Slivnik, L. M. Mir, and D. Miklavcic, "Sequential finite element model of tissue electropermeabilization," *IEEE Trans Biomed Eng*, vol. 52, no. 5, pp. 816–827, 2005, doi: 10.1109/TBME.2005.845212.

[22] A. Zupanic, B. Kos, and D. Miklavcic, "Treatment planning of electroporation-based medical interventions: electrochemotherapy, gene electrotransfer and irreversible electroporation," *Phys Med Biol*, vol. 57, no. 17, pp. 5425–5440, Sep. 2012, doi: 10.1088/0031-9155/57/17/5425.

[23] O. Gallinato, B. D. de Senneville, O. Seror, and C. Poignard, "Numerical workflow of irreversible electroporation for deep-seated tumor," *Physics in Medicine & Biology*, vol. 64, no. 5, p. 055016, Mar. 2019, doi: 10.1088/1361-6560/ab00c4.

[24] G. Pucihar, J. Krmelj, M. Reberšek, T. B. Napotnik, and D. Miklavčič, "Equivalent pulse parameters for electroporation," *IEEE Trans Biomed Eng*, vol. 58, no. 11, pp. 3279–3288, Nov. 2011, doi: 10.1109/TBME.2011.2167232.

[25] S. Z. K. Sajib, O. I. Kwon, H. J. Kim, and E. J. Woo, "Electrodeless conductivity tensor imaging (CTI) using MRI: basic theory and animal experiments," *Biomed Eng Lett*, vol. 8, no. 3, pp. 273–282, Apr. 2018, doi: 10.1007/s13534-018-0066-3.

[26] A. Groselj *et al.*, "Coupling treatment planning with navigation system: a new technological approach in treatment of head and neck tumors by electrochemotherapy," *Biomed Eng Online*, vol. 14 Suppl 3, p. S2, Aug. 2015, doi: 10.1186/1475-925X-14-S3-S2.